文章编号: 1001 - 9014(2019)04 - 0395 - 08

DOI:10.11972/j.issn.1001 - 9014.2019.04.001

Potentials of GaP as millimeter wave IMPATT diode with reference to Si, GaAs and GaN

Janmejaya Pradhan[1*], S K Swain[3], S R Pattnaik[2], G N Dash[3]

(1. College of Engineering Bhubaneswar, Bhubaneswar, Odisha 752024, India;
2. National Institute of Science and Technology, Berhampur, Odisha 761008, India;
3. School of Physics, Sambalpur University, Sambalpur, Odisha 768019, India)

Abstract: This paper presents the simulation results of DC, small-signal and noise properties of GaP based Double Drift Region (DDR) Impact Avalanche Transit Time (IMPATT) diodes. In simulation study we have considered the flat DDR structures of IMPATT diode based on GaP, GaAs, Si and GaN (wurtzite, wz) material. The diodes are designed to operate at the millimeter window frequencies of 94 GHz and 220 GHz. The simulation results of these diodes reveal GaP is a promising material for IMPATT applications based on DDR structure with high break down voltage (V_B) as compared to Si and GaAs IMPATTs. It is also encouraging to worth note GaP base IMPATT diode shows a better output power density of 4.9×10^9 W/m^2 as compared to Si and GaAs based IMPATT diode. But IMPATT diode based on GaN(wz) displays large values of break down voltage, efficiency and power density as compared to Si, GaAs and GaP IMPATTs.

Key words: lmpact avalanche transit time(IMPATT), GaP, GaN, microwave and millimetre wave
PACS: 85.30-z

Introduction

Semiconductors materials and devices have the significant role in effective communication system. In modern technology, the device like Impact Avalanche Transit Time (IMPATT) diode generates stable, economical and reliable RF power at microwave (3 ~ 30 GHz) and millimeter wave (30 ~ 300 GHz) frequencies[1-3]. IMPATT diodes are the most general and commonly used in many aspects of life, as solid state receivers and transmitters, as oscillator for microwave radar receivers, sensor systems etc. IMPATT diodes favour all because these enjoy the flexibility of being fabricated from the narrow bandgap (NBG) semiconductor materials e. g. Ge, Si, InP and GaAs[4-11] and its principle of operation does not depend on any specific physical characteristics of a semiconductor material. Recent development of semiconductor technology has explored the potentiality IMAPTT diodes based on a number of wide bandgap (WBG) semiconductors IMPATT diodes based on 3H-SiC, 4H-SiC, 6H-SiC and GaN are capable of delivering high RF power with significantly high DC to RF conversion efficiency at microwave, mm-wave and terahertz[12-20] frequency regime. In this paper, the authors have explored the potential of another wide bandgap (WBG) semiconductor GaP as a base material for IMPATT diode operating at two different window frequencies of 94 GHz and 220 GHz through a set of computer simulation programs. The simulation results are compared with the Si, GaAs and wurzite(wz) GaN based IMPATT diode.

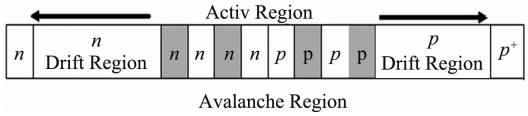


Fig. 1 1-D schematic diagram of the proposed IMPATT diodes

1 Material parameter and design consideration

The material parameters take the vital role for the design of the diodes as well as the IMPATT operation. The values of material parameters of the base semiconductors are the carrier ionization rate, saturation drift velocity of electron (v_{sn}), and hole (v_{sp}), mobility (μ), permittivity (ε_s) etc obtained from the research reports[21-33]. These material parameters are fed for the computer simulation of IMPATT diodes have been summarized in table 1. In addition to these parameters some other factors are required such as the diode area, junction temperature and the operating current density at the desired design frequency. In this case we have taken the u-

Received date: 2018-09-24, **revised date**: 2019-05-05 收稿日期:2018-09-24, 修回日期:2019-05-05
Biography: Janmejaya Pradhan, Ph. D. E-mail: janmejaya74@gmail.com
* **Corresponding author**: E-mail: janmejaya74@gmail.com

niform diode area and junction temperature, but the current density is taken in agreement with the operating frequency. To design an IMPATT diode one needs to consider its efficiency, frequency of operation, low cost, low loss thermal and electrical constants, output power and it is also important to achieve the breakdown condition for IMPATT operation. All the above discussed factors depend upon some basic material properties such as energy band gap, ionization rate, dielectric constant, thermal conductivity, saturation drift velocity of electrons and holes, breakdown electric field etc. Taking into account the suitability of all these material properties, we have used the design criteria as $W_{n,p} = 0.5\ v_{sn,sp}/f_d$, where $W_{n,p}$ the n- or p-side depletion layer widths, and v_sn, $_s$p saturation velocities of electrons/holes. In the present simulation a one-dimensional (1-D) double drift region (DDR) optimized structures of n^+-n-p-p^+ IMPATT diode shown in Fig. 1 is taken into account. It may be assumed without any loss of generality or accuracy, the physical phenomena take place in the semiconductor bulk along the symmetry axis (i.e. x-axis) of the device during IMPATT operation under reverse bias at the frequencies of 94 and 220 GHz. The sum of the width of n-region and p-region is the active region which has been mentioned in the table 2. The width of n^+ and p^+ are negligible and are hence used for ohmic contacts. The doping concentration for each n and p region of all structures have been mentioned in table 2, while the doping concentration for each n^+ and p^+ region are taken as 1.0×10^{26} m^{-3}.

Table 1 Material parameters of Si, GaAs, GaP and GaN (wz) semiconductors

Parameters	Si	GaAs	GaP	GaN(wz)
E_g(eV)	1.12	1.42	2.26	3.4
E_c($\times 10^6$ V/m)	–	0.65	–	5.0
* A_n($\times 10^8$ m^{-1})	0.62	5.6	0.85	250
* B_n($\times 10^8$ Vm^{-1})	1.31	2.41	1.78	34
* A_p($\times 10^8$ m^{-1})	2.0	1.5	0.85	3.48
* B_p($\times 10^8$ Vm^{-1})	2.17	1.57	1.78	18.1
* m	1	1	1.4	1
v_{sn}($\times 10^5$ m/s)	1.05	1.0	1.25	2.5
v_{sp}($\times 10^5$ m/s)	0.81	1.0	1.25	2.5
μ_n($m^2V^{-1}S^{-1}$)	0.058	0.85	0.011	0.046
μ_p($m^2V^{-1}S^{-1}$)	0.04	0.019	0.075	0.012 5
ε (10^{-11} F/m)	10.0	11.4	9.828	8.4

* $\alpha_n = A_n \exp[-(B_n/E)]^m$, $\alpha_p = A_p \exp[-(B_p/E)]^m$

The optimized operating current density, junction temperature and diode area are taken for window frequency of 94 GHz and 220 GHz and listed in table 2. Again the junction temperature and diode area are taken as 300 K and 1.0×10^{-10} m^2 respectively. Though the applications of IMPATT diode are mostly realized on the basis of double drift region structures, the authors have considered the symmetrical double drift region (DDR) IMPATT diode structures with doping distribution of the form n^+ npp$^+$ as shown in table 2 for the dc, small signal and noise analysis. The n^+ and p^+ regions of the diode are heavily doped with each having a doping concentration of 1.0×10^{26} m^{-3}. Each n and p regions has a moderate doping concentration for different materials based on the optimized current density as given in table 2. The total active regions width is taken along with different space points of 1nm each on both p-region and n-region. The values of doping concentrations and diode active region width are taken for optimum conversion efficiency and operation at atmospheric window frequencies of 94 and 220 GHz. The net doping concentration at any space point is hence determined by using the exponential and error function profiles.

2 Computer simulation method

We have first considered the diodes to be consisting of several small space points with a space step of 1 nm. The equations involved have been solved simultaneously at each space point of the active layer of the diode. The DC analysis is carried out by solving simultaneously three important device equations namely Poisson's equation, the carrier continuity equation and the space charge equation using a double iterative DC simulation program. The simulation takes into account the contribution from each space point. It thus efficiently determines DC electric field profiles, carrier current profiles, breakdown voltage etc. for the proposed diodes. The results obtained from DC analysis are used for the high frequency performance analysis of IMPATT diode using a small signal computer simulation method. The small signal model also takes into account the contribution from each space point. The equations are again solved at each space point and it thus effectively determines the device parameters such as negative conductance ($-G$), negative resistance ($-Z_R$) and expected power output (P) of the IMPATT diode. Further, noise is a significant feature in the simulation

Table 2 Design parameters of Si, GaAs, GaP and GaN(wz) DDR IMPATT

f_d/GHz	Materials	Width of active region (nm)		Doping concentrations ($\times 10^{23}$ m^{-3})		J_o($\times 10^8$ Am^{-2})
		n-region (W_n)	p-region (W_p)	n-region N_D	p-region N_A	
94	Si	555	430	0.80	0.85	3.2
	GaAs	530	530	0.65	0.65	2.0
	GaP	660	660	0.63	0.63	2.6
	GaN(wz)	1 320	1 320	1.55	1.55	5.7
220	Si	245	185	2.70	2.75	15.0
	GaAs	225	225	2.00	2.00	7.3
	GaP	284	284	2.10	2.10	12.0
	GaN(wz)	400	400	4.0	4.0	18.5

study of the IMPATT diode. The noise characteristics of the diode structure are computed using a generalized noise simulation program developed by our group. The noise characteristics like mean square noise voltage per band-width (MSNVPBW) and noise measure (NM) of the proposed GaP IMPATT diodes are computed from this analysis. The details of the computer simulation method can be obtained from our previous published report[18]. Our simulation method comprises of DC, small signal and noise analysis. The equations involved in these analyses require complex nonlinear solutions.

3 Result and discussion

The various properties of IMPATT diodes based on the fundamental semiconductor materials like Si, GaAs, Gap and GaN(wz) have been found by our simulation method. The properties like DC characteristics, small signal characteristics and noise behaviors have been computed in DDR structures based on Si, GaAs, Gap and GaN(wz). The details of the results are discussed in the following sections.

3.1 DC characteristics

The computer simulation method has been applied to a DDR structures IMPATT diode based on Si, GaAs and GaP and yields the results of different characteristics. The essential DC characteristics such as peak electric field (E_{max}), breakdown voltage (V_B), avalanche zone voltage (V_A), efficiency (η), avalanche zone width (X_A) and ratio of avalanche zone width to total depletion layer width (X_A/W) of the designed DDR IMPATTs are obtained from DC simulation and presented in table 3. In order to have a comparative description on the prospects of GaP for IMPATT diode with regard to GaAs and Si, the authors have analyzed GaP, GaAs and Si based IMPATT diodes at two different operating frequencies such as 94 and 220 GHz. At both the operating frequencies all the considered IMPATT diodes show different kinds of behavior. From the table 3 it is noticed that, as GaP semiconductor has large band gap as compared to the other two semiconductors, it may show high break down voltage in combination with other properties which have been described in details. The peak electric field profiles and breakdown voltage are computed for all the three IMPATT diodes are presented in table 3. It is observed from the table 3. that at 94 GHz operating frequency the simulated maximum electric fields are 5.63×10^7 V/m, 4.81×10^7 V/m and 4.90×10^7 V/m for GaP, GaAs and Si DDR IMPATT diode respectively. It is noticed that the peak electric field of GaP IMPATT is more as compared with the Si and GaAs IMPATT diodes. At design operating frequencies of 220 GHz, GaP IMPATT diodes show the same trend of higher peak electric field but with increase in design operating frequency the value of peak electric field increases. The electric field profile of the diodes at 94 GHz and 220 GHz operating frequencies are shown in Fig. 2-3 respectively. Since breakdown voltage of IMPATT diodes depends on the value of the peak electric field and diode width, the high value of peak electric field of GaP base IMPATT produces high breakdown voltage with other IMPATT diodes. The breakdown voltage for GaP IMPATT diode shows the high value of 38.99 V whereas the breakdown voltages of GaAs and Si DDR IMPATT are 29.47 and 23.35 V respectively at the same design frequency of 94 GHz and this is due to the difference in peak electric field and the diode width. This value of breakdown voltage of GaP DDR IMPATT structure is about 24.42% more than that of GaAs DDR IMPATT and 40.11% more than that of Si DDR IMPATT structures and hence it produces high RF power output as compared with the other two diodes, which is elucidated in next section. Though GaP has high band gap energy, GaAs IMPATT provides more efficiency than GaP and Si DDR IMPATT and the efficiency values are 11.63 %, 13.26 % and 11.89 % for GaP, GaAs and Si DDR IMPATT diode respectively. At the operating frequency of 220 GHz it can be seen that the computed values of maximum electric fields are 7.20×10^7 V/m, 5.83×10^7 V/m and 6.27×10^7 V/m for GaP, GaAs and Si DDR IMPATT diode respectively. The maximum electric field of all the diodes has been increased with increase in operating frequency. The breakdown voltages of these three considered IMPATT diodes are 21.02 V, 14.91 V and 13.18 V respectively. Si IMPATT shows an efficiency of 9.62% and GaAs IMPATT shows the same of 11.17% whereas for GaP IMPATT efficiency is about 9.91% which is less than that of GaAs DDR IMPATT. It is noticed that the efficiency of all the diode structures decrease with an increase in the operating frequency, at 94 GHz, GaAs shows high efficiency and at 220 GHz gives the low efficiency. Besides the discussed DC properties some of the other DC properties also show the significant behavior and presented in table 3. So far the operating frequency is concerned, it is seen that breakdown voltage values of the DDR IMPATT structures based on GaP, GaAs and Si decrease with increase in operating frequency. At operating frequency of 94 GHz, GaP DDR IMPATT shows 38.99 V whereas at 220 GHz it is 21.02V. Hence one may conclude that with an increase in operating frequency there is a decrease in breakdown voltage.

Table 3 DC properties of Si, GaAs and GaP DDR diodes at 94 and 220 GHz

f_d/GHz	Materials	E_{max}/ $\times10^7$ m^{-1}	V_B/V	V_D/V	(X_A/W) /(%)	η/(%)
94	Si	4.90	23.35	8.72	38.80	11.89
	GaAs	4.81	29.48	12.28	41.42	13.26
	GaP	5.63	38.99	14.25	41.67	11.63
220	Si	6.27	13.18	4.29	45.48	10.36
	GaAs	5.83	14.91	5.44	48.22	11.62
	GaP	7.20	21.02	6.54	44.72	9.91

This happens due to the decrease in active diode width. On the whole it is found that GaAs IMPATTs exhibit the highest efficiency among all the three semiconductors under consideration and GaP base IMPATTs show high breakdown voltage. It is thus interesting to observe that our proposed GaP IMPATT diode exhibits the highest break down voltage along with high peak electric field among all the three diodes under consideration. The percentage of the ratio of avalanche zone width to total drift layer width (X_A/W) for all the diodes under consideration increases with higher operating frequencies. Higher

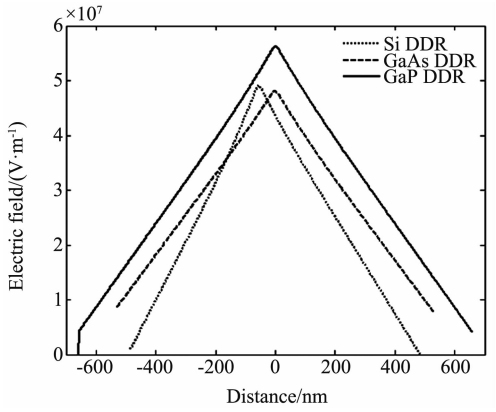


Fig. 2 Electric field profile of DDR IMPATT operating at 94 GHz

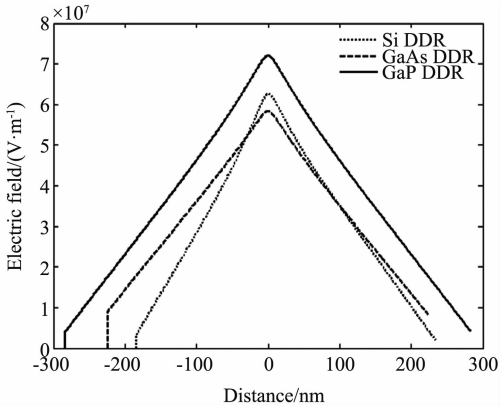


Fig. 3 Electric field profile of DDR IMPATT operating at 220 GHz

X_A/W indicates wider avalanche zone which leads to higher avalanche voltage (V_A) and lower drift zone voltage (V_D). In case of GaAs-based DDRs X_A/W is 42.36 % at 94 GHz but it rises to 48.22 % at 220 GHz which causes the decrease of efficiency (η) at 220 GHz. But in Si DDRs at 94 GHz, X_A/W is 42.7 %, whereas it is 45.48 % at 220 GHz and this leads to fall in efficiency (η) at higher mm-wave frequencies. In case of GaP DDR device the magnitude of X_A/W is much lower up to a frequency of 94 GHz (40.0 %), but it increases rapidly to 44.72 % at 220 GHz this increase in X_A/W with operating frequency yields the fall in efficiency.

3.2 Small signal characteristics

The output of the DC analysis has been used as the input for the simulation of small signal analysis. The significant high-frequency or small signal parameters obtained from this analysis are optimum frequency (f_p), peak negative conductance ($-G_o$), negative resistance (Z_R), RF power output (P_{RF}) and output power density (P_D). These parameters are obtained from the high-frequency simulation of GaP, GaAs and Si DDR IMPATTs at several biased current density and represented in table 4. At operating frequency of 94 GHz, GaP DDR IMPATT diode gives the negative conductance of 1.44×10^7 Sm^{-2}. At the same temperature and operating frequency the negative conductance values of other two IMPATT diodes based on GaAs and Si are 1.9×10^7 Sm^{-2} and 2.55×10^7 Sm^{-2} respectively. It is seen that the negative conductance of Si is more than that of GaAs and GaP diodes. It is also observed that wide band gap semiconductor shows less negative conductance. The diode negative conductance ($-G_o$) as a function of frequency for GaP, GaAs and Si DDR IMPATT are plotted in Fig. 4 and Fig. 5.

Table 4 Small signal characteristics of Si, GaAs and GaP DDR IMPATT diodes at design frequency of 94 and 220 GHz

f_D/GHz	Materials	$-G_o/\times 10^7$ Sm^{-2}	$-Z_R/\times 10^{-9}\Omega m^2$	$P_D/\times 10^9$ Wm^{-2}	P_{RF}
94	Si	2.55	17.3	1.74	1.74
	GaAs	1.91	8.49	2.07	2.07
	GaP	1.44	13.9	2.73	2.73
220	Si	15.6	3.96	3.40	3.40
	GaAs	10.4	1.59	3.92	3.92
	GaP	8.86	3.21	4.90	4.90

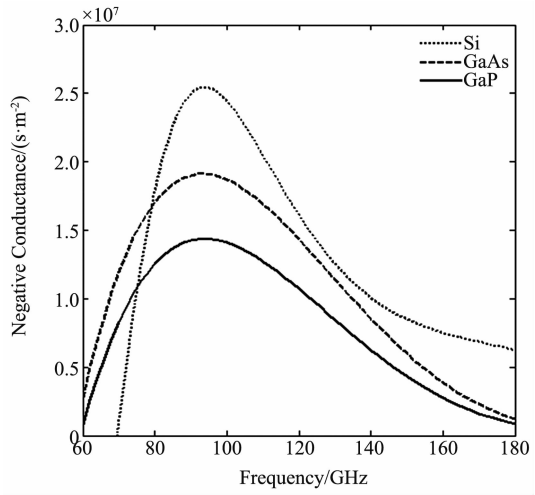


Fig. 4 Variation of negative conductance with frequency for DDR IMPATT operating at 94 GHz

From figures it is observed that, as the diodes are optimized with the current density, the peak of the negative conductance lies at the design operating frequency 94 GHz and 220 GHz, it is noticed that the peak negative conductance of Si is remarkable high recording a value of 2.55×10^7 Sm^{-2}. Subsequently in negative resistance case the behavior is directly reverse. The GaP based IMPATT DDR diode gives more value of negative resistance ($-Z_R$) than that of Si and GaAs DDR diodes. The simulated values of negative resistance of GaP, GaAs and Si DDR IMPATT are of 13.9×10^{-9} Ωm^2, 8.49×10^{-9} Ωm^2 and 17.3×10^{-9} Ωm^2 respectively. The variation of negative resistance with frequency operating at 94 GHz and 220 GHz are plotted in figure 6 and figure 7 and these show that GaP and GaAs base IMPATTs give more negative resistance as compared with Si DDR IMPATT.

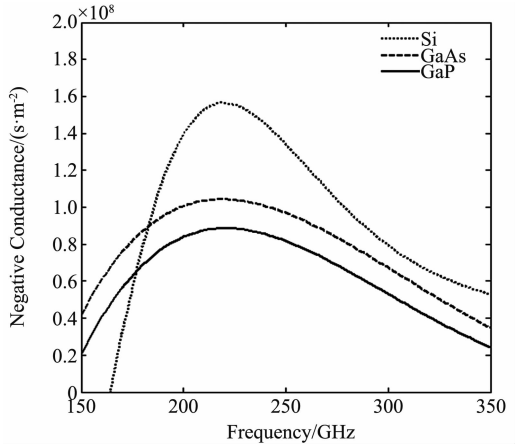


Fig. 5 Variation of negative conductance with frequency for DDR IMPATT operating at 220 GHz

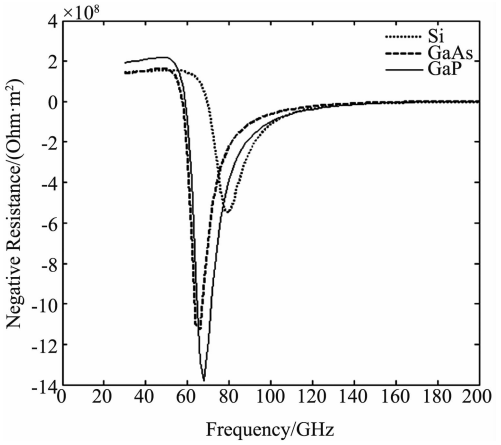


Fig. 6 Variation of negative resistances with frequency for DDR IMPATT diodes operating at 94 GHz

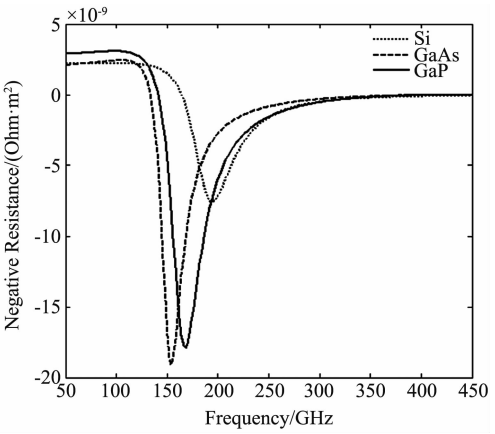


Fig. 7 Variation of negative resistances with frequency for DDR IMPATT diodes operating at 220 GHz

The high breakdown voltage of GaP IMPATT provides large power density. It is found to be 2.73×10^9 W/m^2 for GaP based IMPATT diode which is observed to be nearly two times more than that of Si and GaAs based IMPATT diodes. The high value of power density indicates GaP IMPATT diode is capable of high output power. The simulated output power of GaP, GaAs and Si are 0.273 W, 0.20 W and 0.174 W respectively.

At 220 GHz operating frequency the negative conductance of GaP based DDR IMPATT can be found as 8.86×10^7 Sm^{-2}, which is less than that of Si and GaAs based DDR diodes. For GaAs and Si bas IMPATT the values of negative conductance are 1.04×10^8 Sm^{-2} and 1.56×10^8 Sm^{-2} respectively. The negative resistance values of the three different diodes of Si, GaAs and GaP are 3.96×10^{-9} Ωm^2, 1.59×10^{-9} Ωm^2 and 3.21×10^{-9} Ωm^2 respectively. Using the computed values of breakdown voltage and negative conductance of diodes, the power density of Si, GaAs and GaP, at 220 GHz operating frequency are found to be 3.40×10^9 W/m^2, 3.92×10^9 W/m^2 and $4.90 \times 10^9_{\text{W}}$/m^2 respectively. It is noticed that the power density increases with increase in the operating frequency. It is also notice that whatever be the operating frequency GaP DDR IMPATT diodes show more power density than that of GaAs and Si base DDR IMPATT diodes. The power density of GaP is found as nearly twice more than that of Si and GaAs DDR structures. This high power density of GaP generates more noise in the device which is discussed in the following section.

The RF power output of IMPATT based on GaP as well as the conventional base materials such as Si and GaAs with operating frequency have also been presented in table 4. It is interesting to observe that DDR GaP IMPATT diodes are capable of delivering much higher RF power as compare to their Si and GaAs counterparts at 94 and 220 GHz operating frequencies. Therefore, GaP is the more preferable material over conventional base materials such as Si and GaAs for fabricating DDR IMPATTs especially at higher mm-wave frequencies (220 GHz).

3.3 Noise properties

Since noise is an important aspect of IMPATT study[18-19] the author has analyzed the noise characteristics of GaP IMPATT diode and compared the results with that of GaAs and Si based IMPATT diodes. Mean square noise voltage per band width of the three different diodes based on GaP, GaAs and Si at different operating frequencies of 94 GHz and 220 GHZ as presented in table 5. It is seen that the peak values of mean square noise voltage per band width $(<v^2>/\text{df})_{\max}$ are found at the frequencies (f_p) of 75 GHz and 160 GHz for Si, 60 and 155 GHz for GaAs and 65 GHz and 160 GHz for GaP IMPATT at the operating frequency of 94 and 220 GHz respectively. The corresponding values of mean square voltage per band width ($<v^2>/\text{df}$) at the operating frequency of 94 and 220 GHz for all the diodes are also given in table 5. The simulated values of mean square noise voltage per band width (MSNVPBW) ($<v^2>/\text{df}$) of the diodes around the operating frequency 94 GHz are 1.55×10^{-15} V^{2}s, 5.54×10^{-16} V^{2}s and 1.51×10^{-15} V^{2}s for GaP, GaAs and Si base IMPATT diodes respectively. Similarly, the mean square noise voltage per band width (MSNVPBW) of the diodes at 220 GHz operating frequency show same trend as shown by the diode at 94

GHz. In both the operating frequency GaAs DDR IMPATT shows minimum mean square noise voltage per band width. The variation of mean square noise voltages per bandwidth (MSNVPBW) of the IMPATT diodes based on the semiconductors under consideration as a function of frequency are plotted in figure 8 and figure 9 at the operating frequency of 94 GHz and 220 GHz respectively. It is observed that the GaP based DDR IMPATT diode has the highest ($<v^2>/df$) peak of MSNVPBW compared to the other two diodes. It may also be observed that GaP IMPATT diode is supposed to produce more noise as the value of ($<v^2>/df$) remains high for GaP IMPATT diode. The high value of noise may be understood that GaP IMPATT diode operates under a high electric field as compared to Si and GaAs based IMPATT diodes. The values of computed noise measure (NM) at the designed frequencies are presented in table 5. The noise measure of GaP IMPATT diodes are 28.27 dB and 26.3 dB at the design operating frequencies of 94 and 220 GHz respectively which are larger than that of Si and GaAs base IMPATT diodes. The plots of noise measure as a function of frequency are depicted in Fig. (10 - 11) for all the IMPATT diodes based on GaP, GaAs and Si at different operating frequencies of 94 GHz and 220 GHz. From Fig. (10 -11), it can be seen that the noise measure curve for GaP IMPATT diode is marginally higher as compared to the other two diode structures based on Si and GaAs. IMPATT diode based on GaAs produces less noise as compare to Si and GaP at the operating frequency of 94 and 220 GHz. One important feature of the GaAs IMPATT noise measure is that it is substantially lower than that of Si and GaP based IMPATT diodes. The same electron and hole ionization rates is the key source of low noise behavior of GaAs, whereas in Si the electron and hole ionization rates are quite different this yield higher noise. However, the high power generation mechanism in GaP IMPATT diode yields more noise measure.

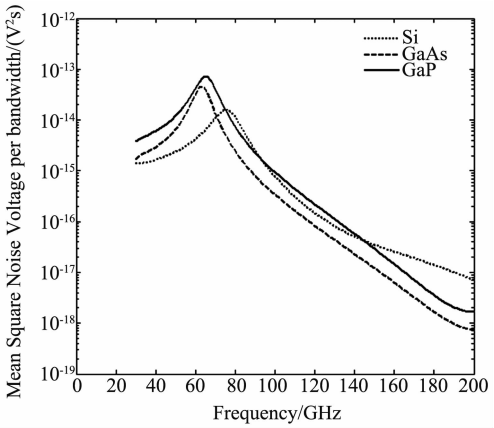


Fig. 8 Variation of mean square voltage per bandwidth with frequency for DDR IMPATT diodes operating at 94 GHz

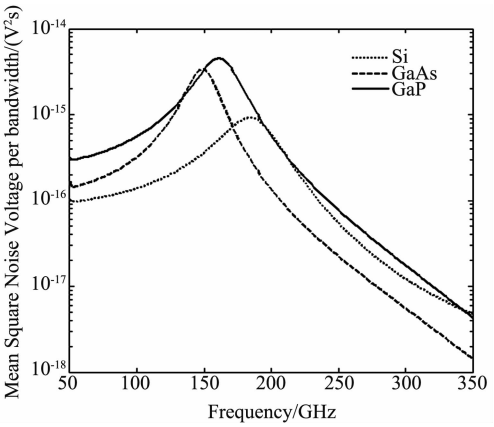


Fig. 9 Variation of mean square voltage per bandwidth with frequency for IMPATT DDR operating at 220 GHz

Table 5 Noise properties of Si, GaAs and GaP, DDR IMPATT diodes

Material	frequency at $(<v^2>/df)_{max}$ (GHz)	$(<v^2>/df)_{max}$ (V^2s)	f_d/GHz	$(<v^2>/df)$ at f_d (V^2s)	NM at f_d /dB
Si	75	1.59×10^{-14}	94	1.51×10^{-15}	27.23
	160	8.95×10^{-16}	220	2.04×10^{-16}	24.94
GaAs	60	4.52×10^{-14}	94	5.54×10^{-16}	25.96
	155	3.40×10^{-15}	220	5.98×10^{-17}	23.55
GaP	65	7.16×10^{-14}	94	1.55×10^{-15}	28.27
	160	4.54×10^{-15}	220	2.27×10^{-16}	26.58

3.4 Comparative study of GaP and GaN (wz) IMPATT

The potential of GaP IMPATT diode has again been compared with another wide bandgap semiconductor GaN (wz) base IMPATT diode and the details are mention in table 6. The electric field and breakdown voltage of GaN (wz) IMPATT diode are around ten times greater than that of GaP IMPATT diode. This predicts that GaP IMPATT can work at low electric field. GaN (wz) IMPATT diodes shows better efficiency than that of GaP IMPATT. The power density of GaN (wz)[14,20] is very large as compared to GaP IMPATT diode. The noise behavior of GaN(wz) IMPATT is quite large as compared to the GaP IMPATT.

4 Conclusion

The potential of millimeter wave DDR GaP IMPATT diode have been explored with a comprehensive DC and small-signal simulation and the simulation results are

Table 6 DC, small signal and noise properties of GaP and GaN(wz) DDR diodes at 94 and 220 GHz

f_d/GHz	Materials	E_{max}/($\times10^7$ Vm^{-1})	V_B/V	η/(%)	$-G_d$/$\times10^7$ Sm^{-2}	P_D/Wm^{-2}	$(<v^2>/df)/(V^2s)$	NM/dB
94	GaP	5.63	38.99	11.63	1.44	2.73×10^9	1.55×10^{-15}	28.27
	GaN(wz)	37.8	527.32	16.95	0.71	2.46×10^{11}	3.81×10^{-14}	38.10
220	GaP	7.20	21.02	9.91	8.86	4.90×10^9	2.27×10^{-16}	26.58
	GaN(wz)	43.40	276.85	16.36	0.31	2.95×10^{11}	2.29×10^{-15}	34.62

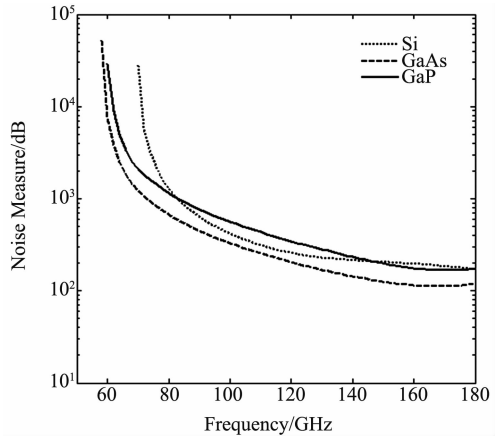


Fig. 10　Variation of noise measure with frequency for DDR IMPATT diodes operating at 94 GHz

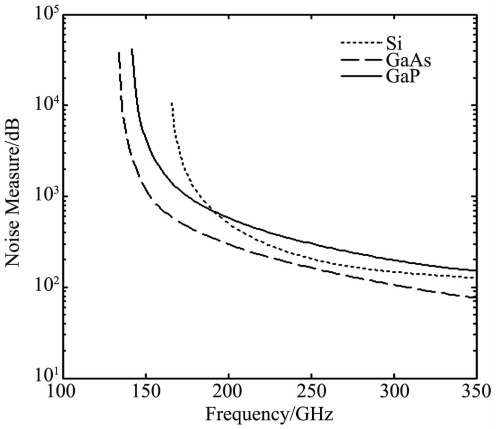


Fig. 11　Variation of noise measure with frequency for DDR IMPATT diodes operating at 220 GHz

compared with narrow bandgap as well as wide bandgap base materials of Si, GaAs and GaN(wz) DDR IMPATT designed to operate at 94 GHz and 220 GHz mm-wave window frequencies. The simulation results show DDR GaP IMPATTs are capable of delivering considerably higher RF power at mm-wave atmospheric window frequencies as compared to their conventional counterparts such as DDR IMPATTs based on Si and GaAs. Thus GaP can be chosen as a base material for IMPATT diode in comparison with that of Si or GaAs. This is supported with the high values of breakdown voltage and high power density. However the diode would produce slightly more noise as compared to GaAs and Si based IMPATT diode. Since IMPATT diodes are meant for high power application GaP would be a good base material for fabrication of IMPATT diode but at the same time care should be taken to reduce the noise. The optimum design parameter and simulation results presented in this paper will be useful for fabrication of mm-wave GaP IMPATT diode by using either molecular beam epitaxy or metalorganic vapor deposition technique. For high electric field one can favor GaN for IMPATT diode over GaP IMPATT diode.

References

[1] Chang L C, Hu D H, Wang C C. Design considerations of high efficiency double drift silicon IMPATT diodes[J]. *IEEE Trans. Electron. Devices*, 1977, **ED-24**: 655 - 657.

[2] Midford T A, Bernick R L. Millimeter wave CW IMPATT diodes and oscillators[J]. *IEEE Trans. Microwave Theory Tech.*, 1979, **27**: 483 - 492.

[3] Chang Y, Hellum J M, Paul J A, *et al*. Millimeter-wave IMPATT sources for communication applications[J]. *IEEE MTT-S International Microwave Symposium Digest*, 1977, pp. 216 - 219.

[4] Luy J F, Casel A, Behr W, *et al*. A 90 GHz double-drift IMPATT diode made with Si MBE[J]. *IEEE Transaction on Electron Devices*, 1987, **34**(5):1084 - 1089.

[5] Dalle C, Rolland P, Leiti G. Flat doping profile double-drift silicon IMPATT for reliable CW high power high efficiency generation in 90 GHz window[J]. *IEEE Transaction on Electron Devices*, 1990, **37**(1): 227 - 236.

[6] Wollitzer M, Bucher J, Schafflr F, *et al*. D-band Si-IMPATT diodes with 300 mW CW output power at 140 GHz[J]. *Electron Lettters*, 1996, **32**(2):122 - 123.

[7] Eisele H. Selective etching technology for 94 GHz, GaAs IMPATT diodes on diamond heat sink[J]. *Solid State Electronics*, 1989, **32**(3): 253 - 257.

[8] Eisele H. GaAs W-band IMPATT diodes for very low noise oscillations[J]. *Electronics Letters*, 1990, **26**(2):109 - 110.

[9] Eisele H, Haddad G I. GaAs single-drift flat IMPATT diodes for CW operation at D-band[J]. *Electronics Letters*, 1992, **28**(23):2176 - 2177.

[10] Tschernitz M, Freyer J. GaAs double-drift Read IMPATT diodes[J]. *Electronics Letters*, 1995, **31**(7): 582 - 583.

[11] Eisele H, Chen C C, Munns G O, *et al*. The potential of InP IMPATT diodes as high-power millimeter wave source: first experimental results[J]. *IEEE MIT-S Iternational Microwave Symp. Digest*, 1996, **2**:529 - 532.

[12] Pradhan J, Swain S K, Pattanaik S R, *et al*. Competence of 4H-SiC IMPATT diode for terahertz application[J]. *Asian Journal of Physics*, 2012, **21**(2):175 - 1778.

[13] Mukherjee M, Mazumder N, Roy S K. α-SiC nanoscale transit-time diodes: performance of the photo-irradiated terahertz sources at elevated temperature[J]. *Semicond. Sci. Technol.* 2010, **25**(5):055008.

[14] Panda A K, Pavlidis D, Alekseev E. DC and high frequency characteristics of GaN based IMPATTs[J]. *IEEE Trans. on Electron devices*, 2001, **48**(4):820 - 823.

[15] Sayed E I, I-Badawy A E, Ibrahim S H. Large signal analysis of P-type GaAs IMPATT diode[C]. *The 12th International Conference on Microelectronics*, *Tehran*, Oct. 31-Nov 2, 2000.

[16] Curow M. Proposed GaAs IMPATT device structure for D-band applications[J]. *Electron. Lett.* 1994, **30**(19):1629 - 1630.

[17] Eisel H, Haddad G I. Enhanced performace of GaAs tunnett oscillators above 100 GH_z through diamond heat sinking and power combining[J]. *IEEE Trans. On microw. Theo and Techn.* 1994, **42**(12): 2498.

[18] Patnaik S R, Dash G R, Mishra J K. Prospects of 6H-SiC for operation as an IMPATT Diode at 140 GHz[J]. *Semiconductor Science and Technology*, 2005, **20**(3):299 - 304.

[19] Pradhan J, Pattanaik S R, Swain S K, *et al*. Low noise wide band gap SiC based IMPATT diodes at sub-millimeter-wave frequencies and at high temperature[J]. *Journal of Semiconductors*, 2014, **35**(3): 034006 - 1 - 6.

[20] M. Mukherjee, S. Banerjee and J. P. Banerjee, "Dynamic Characteristics of III-V and IV-IV Semiconductor Based Transit Time Devices in the Terahertz Regime: A Comparative Analysis" Terahertz Science and Technology, 2010,**3**(3):97 - 108.

[21] Kyuregyan A S, Yurkov S N. Room-temperature avalanche breakdown voltages of Si, Ge, SiC, GaAs, GaP and InP[J]. *Sov. Phys. Semicond.* 1989, **23**(10):1126 - 1132.

[22] Blakemore J S. Semiconducting and other major properties of gallium arsenide[J]. *J. Appl. Phys.*, 1982, **53**(10):R123 - R181.

[23] Pozhela J, Reklaitis A. Electron? transport properties in GaAs at high

electric fields[J]. *Solid State Electron*, 1980, **23**(9):927-933.
[24] Dalal V L, Dreeben A B, Triano A. Temperature dependence of hole velocity in p-GaAs[J]. *J. Appl. Phys.*, 1971, **42**(7):2864-2867.
[25] Pearsall T P, Capasso F, Nahory R E, et al. The band structure dependence of impact ionization by hot carriers in semiconductors, Solid State Electron[J]. 1978, **21**:297-302.
[26] Maes W, De Meyer K, Van Overstraeten R. Impact ionization in silicon[J].? *Solid State Electron.*, 1990, **33**(6):705-718.
[27] Grant W N. Electron? and hole ionization rates in epitaxial silicon at high electric fields[J]. *Solid State Electron.*, 1973, **16**(10): 1189-1203.
[28] Jacoboni C, Canali C, Ottaviani G, *et al*. A review of some charge transport properties of silicon[J]. *Solid State Electron*, 1977, **20**(2), 77-89.
[29] Arora V K, Mui D S L, Morkoc H. High-field electron drift velocity and temperature in gallium phosphide[J]. *Appl. Phys*, 1987,61:4703-4704.
[30] Johnson R H, Eknoyan O. High-field electron drift velocity measurements in gallium phosphide[J]. *J. Appl. Phys*, 1985, **58**(3):1402-1403.
[31] Pradhan J, Swain S K, Pattanaik S R,*et al*. Identification of electron and hole ionization rates in GaAs with reference to IMPATT Diode[J]. *IOSR Journal of Applied Physics* (*IOSR-JAP*), 2012, **2**(1):24-29.
[32] Chen S Y, Wang G. High-field properties of carrier transport in bulk wurtzite GaN: A Monte Carlo perspective[J]. *J. Appl. Phys.* 2008, **103**(2):23703-23708.
[33] Albrecht J D, Wang R P, Ruden P P. Electron transport characteristics of GaN for high temperature device modeling[J]. *J. Appl. Phys.* 1998, **83**(3):4777-4781.